# A simple boundary condition for terminating photonic crystal waveguides

Zhen Hu[1] and Ya Yan Lu[2]

[1]*Department of Mathematics, Hohai University, Nanjing, Jiangsu, China*

[2]*Department of Mathematics, City University of Hong Kong, Kowloon, Hong Kong*

Many photonic crystal (PhC) devices are non-periodic structures due to the introduced defects in an otherwise perfectly periodic PhC, and they are often connected by PhC waveguides that serve as input and output ports. Numerical simulation of a PhC device requires boundary conditions to terminate PhC waveguides that extend to infinity. The rigorous boundary condition for terminating a PhC waveguide is a non-local condition that connects the wave field on the entire surface (or line in two-dimensional problems) transverse to the waveguide axis, and it is relatively difficult to use, especially for realistic devices, such as those in PhC slabs. In this paper, a simple approximate boundary condition involving a few points in the waveguide axis direction is introduced. The new boundary condition is used with the Dirichlet-to-Neumann map method to take advantage of the lattice structures and identical unit cells in PhC devices. Comparisons with the rigorous non-local boundary condition indicate that the simple boundary condition gives accurate solutions if the computational domain is enlarged by a few lattice constants in each direction. 

## 1. Introduction

Photonic crystals (PhCs) [1, 2] have the potential to provide compact and low-loss components for integrated optical circuits. Efficient numerical methods are needed to find optimal designs for PhC components and devices, such as waveguides, cavities, power splitters, channel drop filters, interferometers, etc. Although PhCs are periodic, a typical PhC device is a non-periodic structure due to the various defects that comprise the device. Unlike band structure calculations that are formulated on a unit cell, the numerical simulation of a PhC device is a boundary value problem that involves many unit cells. In particular, PhC devices are often connected by PhC waveguides that serve as input and output ports. Practical numerical simulation for such a device can only be performed in a finite computational domain.

Artificial boundary conditions are needed on the boundary of the computational domain that terminates the PhC waveguides. These boundary conditions must properly model the incoming and outgoing waves in the waveguides.

The finite-difference time-domain method (FDTD) [3] is the most widely used method for simulating light waves in PhC devices, but it requires a small grid size to resolve material interfaces with high index contrast, and a small time step to maintain numerical stability. The frequency-domain finite element method (FEM) [4] is another powerful general method, but it gives rise to large linear systems that are expensive to solve. Both methods also have difficulties for terminating PhC waveguides that extend to infinity, since the widely used perfectly matched layer (PML) [5,6] technique is not effective for terminating extended periodic structures. More efficient numerical methods for PhC devices can be developed by taking advantage of some physical and geometric features. The boundary integral equation (BIE) method is suitable for structures with piecewise constant refractive index profiles. The multipole method [7–11] is suitable for structures containing circular inclusions (dielectric rods or air holes). The Dirichlet-to-Neumann (DtN) map method [12, 13] is an efficient numerical method for two-dimensional (2D) PhC devices. It can take advantage of the identical unit cells and the lattice structure of a typical PhC device. The DtN map of unit cell is a relation between a wave field component and its normal derivative on the cell boundary. It is the same for all identical unit cells even though the wave fields on these cells are different. The DtN map method solves the wave field on the boundaries of the unit cells only. Unlike the BIE and multipole methods, the DtN map method gives rise to sparse linear systems that can be more efficiently solved. Meanwhile, a rigorous boundary condition for terminating PhC waveguides is available [12]. However, it is a non-local condition, since it connects the wave field in different unit cells perpendicular to the waveguide axis. For pure 2D structures that are invariant in one direction, the non-locality is not a serious drawback, but for three-dimensional (3D) structures such as PhC slabs, the non-local boundary condition becomes too expensive to use.

In this paper, we develop a simple boundary condition for terminating PhC waveguides. It is an approximate boundary condition derived from the asymptotic behavior of waves in the waveguide. The new boundary condition is presented in Section 2 and validated by numerical examples in Section 3.

## 2. DtN map method and boundary conditions

We consider devices in a 2D PhC consisting of infinitely long and parallel dielectric rods on a square lattice and surrounded by a homogeneous medium. Such a PhC is highly idealized, but it has been used to illustrate many interesting properties and potential applications. For the $E$ polarization, if the dielectric rods are parallel to the $z$ axis, then the $z$ component of

the electric field, denoted by $u$ in this paper, satisfies the following Helmholtz equation

$$\partial_x^2 u + \partial_y^2 u + k_0^2 n^2(x,y) u = 0, \tag{1}$$

where $k_0$ is the free space wavenumber and $n(x,y)$ is the refractive index function. As a simple example, an un-optimized 90° bend is shown in Fig. 1, where the PhC is assumed to

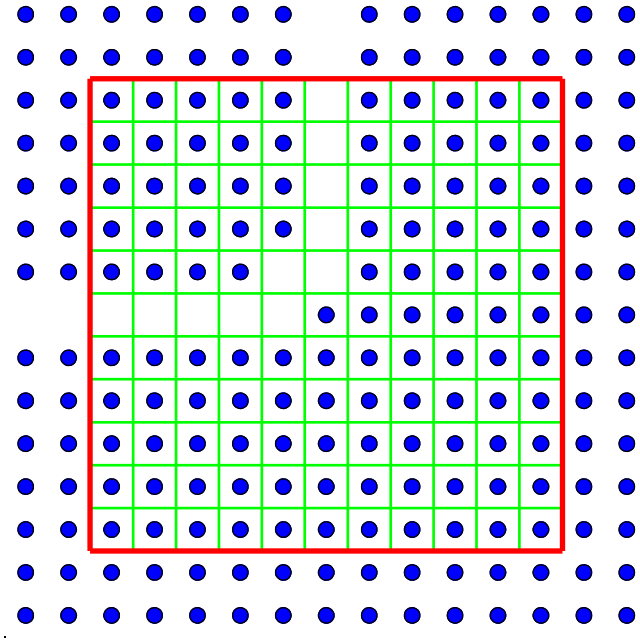

Fig. 1. A 90° bend in a 2D photonic crystal and a truncated domain with $11 \times 11$ unit cells.

be unbounded in the $xy$ plane, and the PhC waveguide, formed by removing a line of rods, extends to infinity in the negative $x$ and positive $y$ directions. To analyze the 90° bend by a numerical method, it is necessary to truncate the $xy$ plane to a bounded computational domain, for example, a square with $m \times m$ unit cells. A truncated domain with $11 \times 11$ unit cells is shown in Fig. 1. The unit cells are squares with side length $a$, where $a$ is the lattice constant of the PhC. Notice that there are only two different types of unit cells: the regular unit cell with a rod inside and the "defect" unit cell which is empty. If the lower-left corner of the truncated domain is $(x_0, y_0)$, then the unit cells are $\Omega_{jk} = \{(x,y) \mid x_{j-1} < x < x_j,\ y_{k-1} < y < y_k\}$ for $1 \le j,k \le m$, where $x_j = x_0 + ja$ and $y_k = y_0 + ka$.

For the unit cell $\Omega_{jk}$, we can calculate the DtN operator $\Lambda^{(jk)}$ that maps $u$ to the normal

derivative of $u$ on the boundary of $\Omega_{jk}$, i.e.,

$$\Lambda^{(jk)} \begin{bmatrix} v_{j-1,k} \\ h_{j,k-1} \\ v_{jk} \\ h_{jk} \end{bmatrix} = \begin{bmatrix} \partial_x v_{j-1,k} \\ \partial_y h_{j,k-1} \\ \partial_x v_{jk} \\ \partial_y h_{jk} \end{bmatrix}, \tag{2}$$

where $v_{jk} = u(x_j, y)$ for $y_{k-1} < y < y_k$, $h_{jk} = u(x, y_k)$ for $x_{j-1} < x < x_j$, $\partial_x v_{jk} = \partial_x u(x_j, y)$ for $y_{k-1} < y < y_k$, etc. A method for constructing matrix approximations of $\Lambda^{(jk)}$ is given in Refs. [14,15]. It relies on approximating the general solution of Eq. (1) in $\Omega_{jk}$ as a sum of $4N$ special solutions, and evaluating the general solution and its normal derivative at $4N$ points on the boundary of $\Omega_{jk}$, where $N$ is the number of sampling point on each edge of the unit cell. In that case, $\Lambda^{(jk)}$ is approximated by a $(4N) \times (4N)$ matrix. In the following, we also need to write $\Lambda^{(jk)}$ in $4 \times 4$ blocks where each block is an $N \times N$ matrix. Based on the DtN maps of the unit cells, we can establish an equation for each edge between two neighboring unit cells by matching the normal derivative of $u$. For example, the common edge of $\Omega_{11}$ and $\Omega_{21}$ is the third edge of $\Omega_{11}$ and the first edge of $\Omega_{21}$ following the ordering implicitly defined in Eq. (2). On that edge, $u$ is denoted as $v_{11}$, and its $x$ derivative $\partial_x v_{11}$ can be evaluated by either $\Lambda^{(11)}$ or $\Lambda^{(21)}$. This leads to

$$\Lambda^{(11)}_{31} v_{01} + \Lambda^{(11)}_{32} h_{10} + \Lambda^{(11)}_{33} v_{11} + \Lambda^{(11)}_{34} h_{11} = \Lambda^{(21)}_{11} v_{11} + \Lambda^{(21)}_{12} h_{20} + \Lambda^{(21)}_{13} v_{21} + \Lambda^{(21)}_{13} h_{21}, \tag{3}$$

where $\Lambda^{(11)}_{31}$, $\Lambda^{(11)}_{32}$, $\Lambda^{(11)}_{33}$ and $\Lambda^{(11)}_{34}$ are blocks of $\Lambda^{(11)}$ in the third row, and $\Lambda^{(21)}_{11}$, $\Lambda^{(21)}_{12}$, $\Lambda^{(21)}_{13}$ and $\Lambda^{(21)}_{14}$ are the blocks of $\Lambda^{(21)}$ in the first row. Putting all equations like the one above together, we obtain a linear system for $u$ on the edges of the unit cells only. This linear system is sparse, since Eq. (3) is only related to the seven edges of the two unit cells. But to complete the problem, we need boundary conditions.

If the frequency is in a bandgap of the PhC, light decays exponentially away from the waveguide core. Therefore, we can use the approximate boundary condition $u = 0$ on the lower and right sides of the truncated domain in Fig. 1. On the top and left sides, artificial boundary conditions are needed to model the incoming and outgoing waves in the semi-infinite waveguides. A rigorous boundary condition [12, 16, 17] for the left side is given as

$$\partial_x u = \mathcal{L}^- u + (\mathcal{L}^+ - \mathcal{L}^-) u^{(inc)}, \quad x = x_0, \tag{4}$$

where $u^{(inc)}$ is the incoming wave (from $x = -\infty$) in the horizontal waveguide, $\mathcal{L}^+$ and $\mathcal{L}^-$ are operators that act on functions of $y$. These operators can be written down if we decompose the wave field in the left waveguide as $u = u^{(inc)} + u^-$ where $u^-$ is the unknown outgoing wave, and expand $u^-$ in Bloch modes of the PhC waveguide [12]. Note that the expansion should include both propagating and evanescent modes, where the propagating modes must

be outgoing (i.e. carry power to $x = -\infty$) and the evanescent modes decay as $x \to -\infty$. When $y$ is discretized, the operators $\mathcal{L}^{\pm}$ are approximated by $(mN) \times (mN)$ matrices, where $m$ and $N$ are integers given above. Notice that the boundary condition (4) is non-local, since it connects $u$ for all $y$ ($y_0 < y < y_m$) together.

A much simpler but approximate boundary condition can be derived, if we assume that the left side $x = x_0$ is sufficiently far away from the center of the bend, so that the evanescent Bloch modes are small enough at $x_0$ and the field in the horizontal waveguide for $x \leq x_0$ can be approximated by propagating Bloch modes only. That is

$$u \approx u^{(inc)} + \sum_{l=1}^{l_*} b_l \phi_l^-(x,y) e^{-i\beta_l x}, \tag{5}$$

where $l_*$ is the total number of propagating Bloch mode of the horizontal waveguide, $\phi_l^-(x,y)e^{-i\beta_l x}$ is an outgoing propagating Bloch mode that propagates to $x = -\infty$, $\phi_l^-$ is periodic in $x$ with period $a$, $\beta_l$ is the real propagation constant and $b_l$ is an unknown coefficient. Typically, $u^{(inc)}$ consists of only one incoming Bloch mode, that is, $u^{(inc)} = \phi_1^+(x,y)e^{i\beta_1 x}$. Notice that $\phi_l^+$ and $\phi_l^-$ are the periodic envelopes of the incoming and outgoing Bloch modes with the same propagation constant $\beta_l$.

The simple boundary condition is derived by eliminating the unknown coefficients $\{b_l : 1 \leq l \leq l_*\}$. Consider the following polynomial of $\xi$,

$$\prod_{l=1}^{l_*}(1 - \xi e^{i\beta_l a}) = 1 + B_1\xi + B_2\xi^2 + ... + B_{l_*}\xi^{l_*}.$$

If $w(x,y) = \phi_l^-(x,y)e^{-i\beta_l x}$ is an outgoing propagating Bloch mode, then

$$w_j = w(x_j, y) = e^{-i\beta_l j a} w(x_0, y) = (e^{-i\beta_l a})^j w_0.$$

Since $e^{-i\beta_l a}$ is a zero of the above polynomial, we have

$$w_0 + B_1 w_1 + B_2 w_2 + ... + B_{l_*} w_{l_*} = 0.$$

This leads to the following boundary condition

$$u_0 + B_1 u_1 + ... + B_{l_*} u_{l_*} = u_0^{(inc)} + B_1 u_1^{(inc)} + ... + B_{l_*} u_{l_*}^{(inc)}, \tag{6}$$

where $u_j$ and $u_j^{(inc)}$ denote $u(x_j, y)$ and $u^{(inc)}(x_j, y)$, respectively. If there is no incoming wave in the horizontal waveguide, then Eq. (6) has a zero right hand side. If the horizontal waveguide has only one propagating Bloch mode, then Eq. (6) is reduced to

$$u_0 - e^{i\beta_1 a} u_1 = u_0^{(inc)} - e^{i\beta_1 a} u_1^{(inc)}. \tag{7}$$

Notice that Eq. (6) is a relation for $u$ at a few points and it is independent of $y$. Since a typical PhC waveguide has only a small number of propagating Bloch modes, the boundary

condition (6) it is much easier to use than the non-local boundary condition (4). Of course, it is still necessary to calculate the propagating modes of the PhC waveguide. This can be done efficiently using the DtN formalism [18, 19], even for 3D waveguides [20]. Besides, the boundary condition (6) involves only the propagation constants of these modes.

## 3. Numerical examples

In this section, we illustrate the simple boundary condition (6) by a few numerical examples. First, we consider the un-optimized 90° waveguide bend as shown in Fig. 1. The background PhC is a square lattice of dielectric rods surrounded by air, where the dielectric constant and the radius of the rods are $\varepsilon = 11.56$ and $r = 0.18a$, respectively. For the $E$ polarization, the PhC has a band gap given by $0.302 < \omega a/(2\pi c) < 0.443$. The waveguide formed by removing a line of rods has a single propagating mode for $0.312 < \omega a/(2\pi c) < 0.443$. The structure has been analyzed previously by a number of authors using FDTD [21], FEM [22], the multiple multipole method [23] and the DtN map method with non-local boundary conditions [12]. In particular, the results given in [12, 22, 23] agree well with each other and are believed to be accurate.

We use this example to validate the new boundary condition. For that purpose, we take $\omega a/(2\pi c) = 0.34$, and calculate the transmission coefficient for a given incident wave (an incoming propagating mode) in the horizontal waveguide. To find an accurate reference solution, we repeat the calculation using the DtN map method with the non-local boundary condition for different values of $m$ and $N$, where $m$ is the size of the truncated domain (a square with $m \times m$ unit cells) and $N$ is the number of discretization points on each edge of the unit cells. For $m = 11$ and $N = 9$, the transmission coefficient is $T = 0.9931$. The results for larger $m$ and/or $N$ have the same four significant digits. Using the same $N$ and the new boundary condition, we obtain $T = 0.9941$, $T = 0.9933$ and $T = 0.9931$ for $m = 11$, 13 and 15, respectively. Therefore, with $m = 15$ and the new boundary condition, we are able to reproduce the solution correct to four digits. To obtain three correct digits, i.e., $T = 0.993$, we need only $N = 5$. In that case, the DtN map method requires $m = 11$ and $m = 13$ for the non-local and new boundary conditions, respectively.

To test the simple boundary condition for multi-mode waveguides, we consider the 90° bend in a different PhC, where the dielectric constant and the radius of the rods are $\varepsilon = 10$ and $r = 0.375a$, respectively. At $\omega a/(2\pi c) = 0.785$, the waveguide in this PhC (obtained by removing one row of rods) has one even mode and one odd mode [18,24]. The scaled propagation constants of these two modes are $\beta_1 a/(2\pi c) = -0.3019$ and $\beta_2 a/(2\pi c) = 0.1210$, respectively. Although these two modes have different symmetries, the bend causes mode coupling. As in the first example, we calculate the transmission coefficient for the un-optimized 90° bend with an even incoming mode in the horizontal waveguide. With the non-local boundary

condition, a solution with four correct digits $T = 0.5460$ can be obtained with $m = 11$ and $N = 18$. Here $T$ is the total transmitted power carried by the two modes assuming that the incident wave has unit power. In fact, the transmitted powers carried by the even and odd modes are $T_1 = 0.4294$ and $T_2 = 0.1166$, respectively. The total reflected power $R = 0.4540$ is similarly distributed to the two modes. Using the same $N$ and the simple boundary condition, we obtain $T = 0.5351$, 0.5429, 0.5452, 0.5458 and 0.5460 for $m = 11$, 13, 15, 17 and 19, respectively. Therefore, the new boundary condition gives the correct four digits with $m = 19$. For three correct digits, i.e., $T = 0.546$, we only need $N = 13$. In that case, the non-local and new boundary conditions require $m = 11$ and $m = 17$, respectively.

Finally, we consider T-junctions in a square lattice PhC where the dielectric constant and the radius of the rods are $\varepsilon = 11.56$ and $r = 0.2a$. Fan *et al.* [25] proposed a T-junction with two small extra rods (marked in red) of radius $r_t$ as in Fig. 2(a), where the horizontal

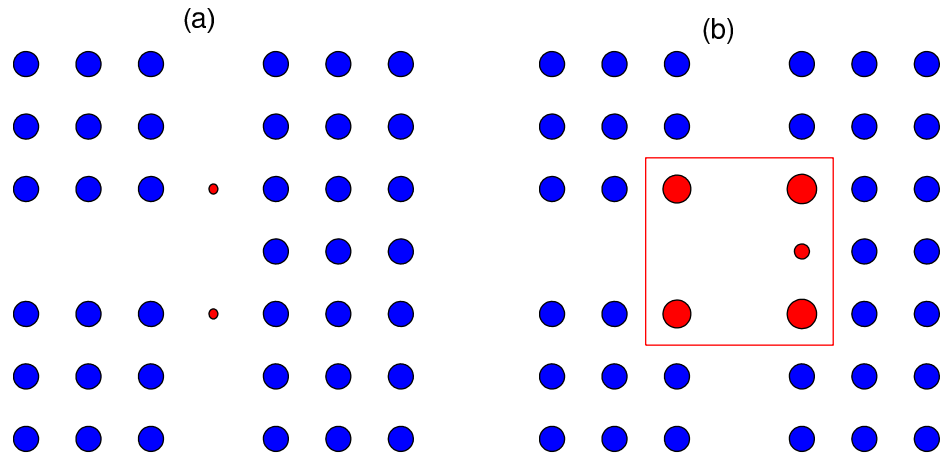


Fig. 2. T-junctions in a PhC with a square lattice of rods. (a) a T-junction of Fan *et al.* [25], (b) an optimized T-junction for high transmission in a large frequency range.

semi-infinite waveguide is the input waveguide, and the two vertical semi-infinite waveguides are the output waveguides. They conclude that this T-junction has high transmission in a small frequency range if $r_t = 0.07a$ and acceptable transmission in a large frequency range if $r_t = 0.03a$. We consider the T-junction shown in Fig. 2(b), where the five rods (marked in red) are allowed to have different radii (but the same dielectric constant and fixed locations), and optimize this structure for broadband operation by maximizing the minimum transmission over a given frequency range. Due to the symmetry between the two output waveguides, the two lower red rods are identical to the two upper red rods. This leads to an optimization problem with three free parameters (the radii of three distinct red rods). The optimization is

carried out by the popular BFGS quasi-Newton method [26]. The DtN map method is used to compute the transmission coefficients in each iteration. We consider two cases using two different frequency intervals. For the frequency range $0.37 \leq \omega a/(2\pi c) \leq 0.42$, the radii of the three red rods of the optimized T-junction are $0.1684a$, $0.2251a$ and $0.0818a$, respectively. The transmission spectra (for each output waveguide) is shown in Fig. 3(a). For comparison,

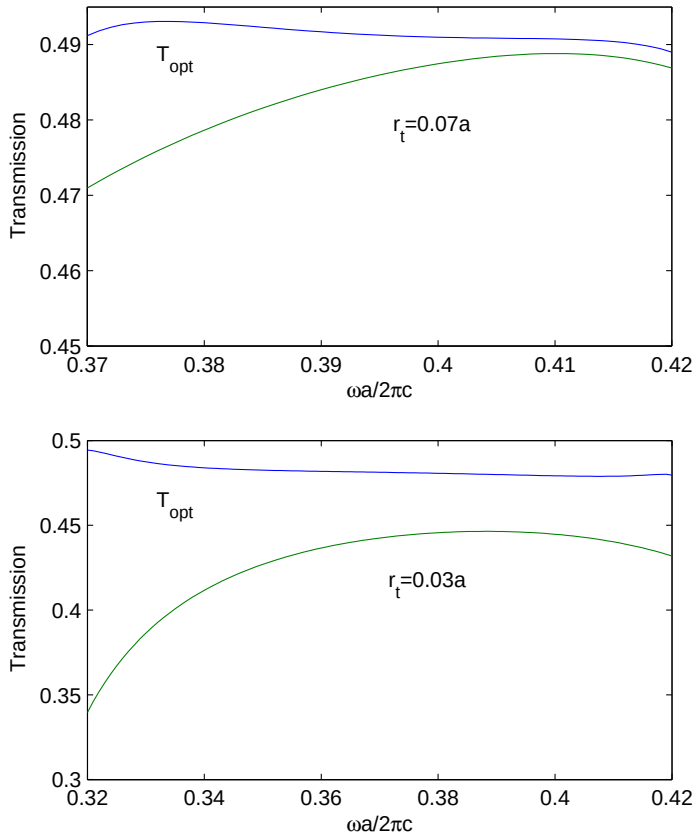


Fig. 3. (a) Transmission spectra of the first optimized T-junction ($T_{opt}$) and the T-junction in [25] with $r_t = 0.07a$. (b) Transmission spectra of the second optimized T-junction ($T_{opt}$) and the T-junction in [25] with $r_t = 0.03a$.

we also show the transmission spectrum for the T-junction of Fan *et al.* [25] with $r_t = 0.07a$. The second case is concerned with a wider frequency interval $\omega a/(2\pi c) \in [0.32, 0.42]$. The optimized T-junction is shown in Fig. 2(b), where the radii of the three red rods are $0.2224a$, $0.2350a$ and $0.1196a$, respectively. In Fig. 3(b), we show the transmission spectra of our T-junction as well as the one given in [25] for $r_t = 0.03a$. To illustrate the operation of our T-junction, we show the electric field patterns at selected frequencies in Fig. 4.

Both non-local and simple boundary conditions are used to compute the transmission

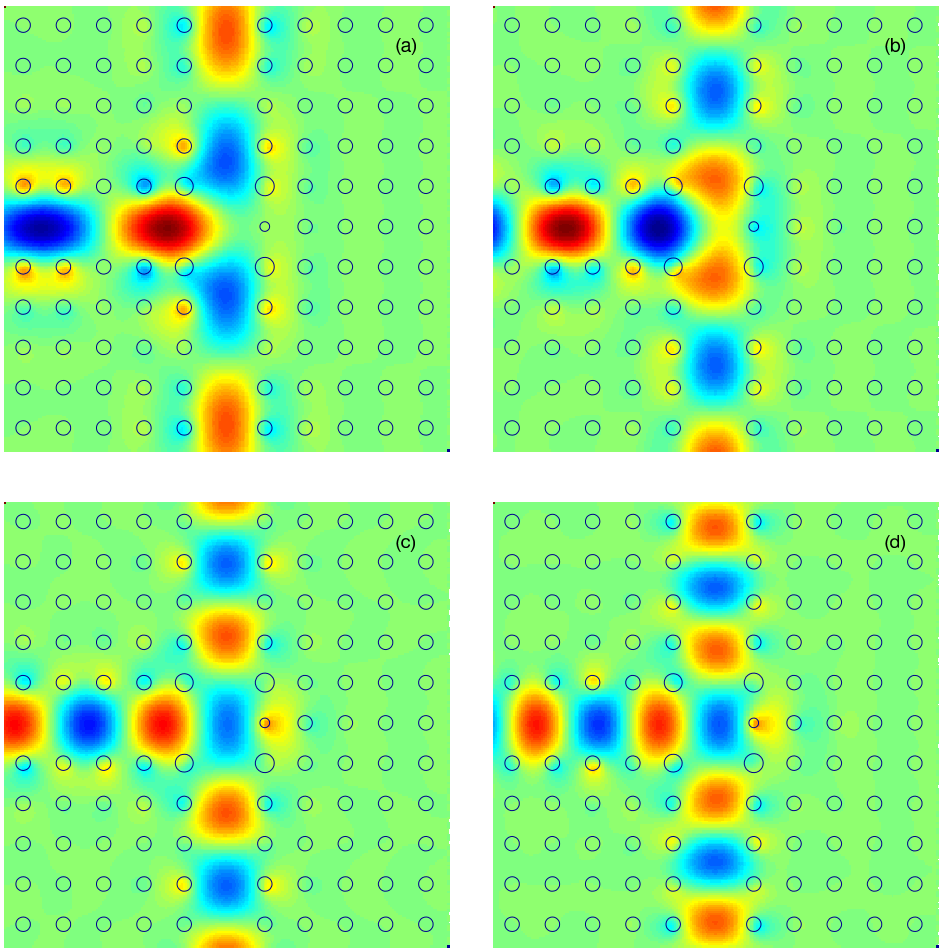


Fig. 4. Electric field patterns for the second optimized T-junction. Panels (a), (b), (c) and (d) correspond to $\omega a/(2\pi c) = 0.33$, 0.35, 0.38 and 0.41, respectively.

coefficients of the optimized T-junctions. For example, if $\omega a/(2\pi c) = 0.38$, the transmission coefficient for each output waveguide is $T = 0.4785$. This result can be obtained with $N = 11$, and $m = 11$ or $m = 13$ for the non-local and simple boundary conditions, respectively.

## 4. Conclusion

Numerical simulations are essential in the design and optimization of PhC devices. For both general numerical methods such as the FDTD and the FEM, and more special methods such as the multipole method and the Dirichlet-to-Neumann map method, boundary conditions are needed to terminate PhC waveguides that serve as input and output ports of the device. These boundary conditions must properly model the incoming and outgoing Bloch modes in

the PhC waveguide. The PML is a popular method for terminating homogeneous or layered media, but it does not work for PhC waveguides. In fact, a PML corresponds to a complex coordinate transform that amplifies (damps) the incoming (outgoing) plane waves exponentially, but it cannot separate incoming and outgoing Bloch modes. A rigorous boundary condition for terminating PhC waveguides was established in earlier works [12, 16, 17], but it is a non-local condition that partially destroys the sparsity of the final linear system, and it is expensive to use for 3D structures in PhC slabs [27]. A simple boundary condition for terminating PhC waveguides is developed and validated in this paper, in connection with the DtN map method that solves only the wave field on the boundaries of the unit cells. The new boundary condition is very simple to implement and it preserves the sparsity of the final linear system. The drawback is that it is only an approximate condition. It requires larger computational domains than the rigorous non-local condition, since it assume that the evanescent Bloch modes in the PhC waveguide can be ignored. Although the new boundary condition is developed for PhC waveguides, it may find applications in other periodic media [28]. Overall, the new boundary condition is a simple alternative that is useful in modeling complex PhC devices.

**Acknowledgement**

This research was partially supported by the National Science Foundation of China (Project No. 11101122), the Fundamental Research Funds for the Central Universities of China (Project No. 2009B05514), and the Research Grants Council of Hong Kong Special Administrative Region, China (Project No. CityU 102411).

**References**

1. J. D. Joannopoulos, S. G. Johnson, J. N. Winn, and R. D. Meade, Photonic Crystals: Molding the Flow of Light, 2nd Ed. (Princeton University Press, Princeton, NJ, 2008).
2. D. W. Prather, S. Shi, A. Sharkawy, and G. J. Schneider, Photonic Crystals: Theory, Applications, and Fabrication, (John Wiley & Sons, Hoboken, NJ 2009).
3. A. Taflove and S. C. Hagness, Computational Electrodynamics: the Finite-difference Time-domain Method, 2nd Ed., (Artech House, Boston, 2000).
4. J. Jin, The Finite Element Method in Electromagnetics, 2nd Ed. (John Wiley & Sons, New York, 2002).
5. J. Berenger, "A perfectly matched layer for the absorption of electromagnetic waves," J. Comput. Phys. **114**, 185-200 (1994).
6. W. C. Chew and W. H. Weedon, "A 3-D perfectly matched medium from modified maxwell's equations with stretching coordinates," Micro. Opt. Tech. Lett. **7**, 599-604 (1994).

7. G. O. Olaofe, "Scattering by an arbitrary configuration of parallel circular cylinders," J. Opt. Soc. Am. **60**, 12331236 (1970).
8. D. Felbacq, G. Tayeb and D. Maystre, "Scattering by a random set of parallel cylinders," J. Opt. Soc. Am. A **11**, 2526-2538 (1994).
9. G. Tayeb and D. Maystre, "Rigorous theoretical study of finite-size two-dimensional photonic crystals doped by microcavities," J. Opt. Soc. Am. A **14**, 3323-3332 (1997).
10. J. Yonekura, M. Ikeda and T. Baba, "Analysis of finite 2-D photonic crystals of columns and lightwave devices using the scattering matrix method," J. Lightwave Technol. **17**, 1500-1508 (1999).
11. P. A. Martin, *Multiple Scattering* (Cambridge University Press, Cambridge, UK, 2006).
12. Z. Hu and Y. Y. Lu, "Efficient analysis of photonic crystal devices by Dirichlet-to-Neumann maps," Opt. Express **16**, 17383-17399 (2008).
13. Z. Hu and Y. Y. Lu, "Improved Dirichlet-to-Neumann map method for modeling extended photonic crystal devices," Opt. Quant. Electron. **40**, 921-932 (2008).
14. Y. Huang and Y. Y. Lu, "Scattering from periodic arrays of cylinders by Dirichlet-to-Neumann maps," J. Lightwave Technol. **24**, 3448-3453 (2006).
15. J. Yuan, Y. Y. Lu and X. Antoine, "Modeling photonic crystals by boundary integral equations and Dirichlet-to-Neumann maps," J. Comput. Phys. **227**, 4617-3629 (2008).
16. P. Joly, J.-R. Li, and S. Fliss, "Exact boundary conditions for periodic waveguides containing a local perturbation," Commun. Comput. Phys. **1**, 945-973 (2006).
17. M. Ehrhardt, J.G. Sun and C. Zheng, "Evaluation of scattering operators for semi-infinite periodic arrays," Commun. Math. Sci. **7**, 347-364 (2009).
18. Y. Huang, Y. Y. Lu and S. Li, "Analyzing photonic crystal waveguides by Dirichlet-to-Neumann maps," J. Opt. Soc. Am. B **24**, 2860-2867, (2007).
19. S. Li and Y. Y. Lu, "Efficient method for computing leaky modes in two-dimensional photonic crystal waveguides," J. Lightwave Technol. **28**, 978-983 (2010).
20. L. Yuan and Y. Y. Lu, "An efficient numerical method for analyzing photonic crystal slab waveguides," J. Opt. Soc. Am. B **28**, 2265-2270 (2011).
21. A. Mekis, J. C. Chen, I. Kurland, S. H. Fan, P. R. Villeneuve and J. D. Joannopoulos, "High transmission through sharp bends in photonic crystal waveguides," Phys. Rev. Lett. **77**, 3787-3790 (1996).
22. M. Koshiba, Y. Tsuji and M. Hikari, "Time-domain beam propagation method and its application to photonic crystal circuits," J. Lightwave Technol. **18**, 102-110 (2000).
23. J. Smajic, C. Hafner and D. Erni, "Design and optimization of an achromatic photonic crystal bend," Opt. Express **11**, 1378-1384 (2003).
24. C. P. Yu and H. C. Chang, "Applications of the finite difference mode solution method to photonic crystal structures," Opt. Quantum Electron. **36**, 145-163 (2004).

25. S. H. Fan, S. G. Johnson, J. D. Joannopoulos, C. Manolatou, and H. A. Haus, "Waveguide branches in photonic crystals," J. Opt. Soc. Am. B **18**, 162-165 (2001).
26. J. Nocedal and S. J. Wright, Numerical Optimization, 2nd Ed. (Springer-Verlag, Berlin, New York, 2006).
27. L. Yuan and Y. Y. Lu, "Dirichlet-to-Neumann map method for analyzing hole arrays in a slab," J. Opt. Soc. Am. B **27**, 2568-2579 (2010).
28. M. Ehrhardt (ed.), Wave Propagation in Periodic Media - Analysis, Numerical Techniques and practical Applications (Progress in Computational Physics, Volume 1, Bentham Science, 2010).